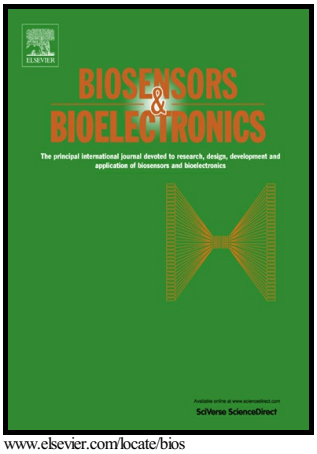

www.elsevier.com/locate/bios

A sensitive photoelectrochemical immunoassay of N^6 - methyladenosine based on dual-signal amplification strategy: Ru doped in SiO_2 nanosphere and carboxylated g-C_3N_4

Haiyan Wang, Chunling Qi, Wenhuan He, Minghui Wang, Wenjing Jiang, Huanshun Yin, Shiyun Ai

PII: S0956-5663(17)30491-8
DOI: http://dx.doi.org/10.1016/j.bios.2017.07.042
Reference: BIOS9875

To appear in: *Biosensors and Bioelectronic*

Received date: 23 May 2017
Revised date: 4 July 2017
Accepted date: 16 July 2017

Cite this article as: Haiyan Wang, Chunling Qi, Wenhuan He, Minghui Wang, Wenjing Jiang, Huanshun Yin and Shiyun Ai, A sensitive photoelectrochemical immunoassay of N^6 - methyladenosine based on dual-signal amplificatio strategy: Ru doped in SiO_2 nanosphere and carboxylated g-C_3N_4, *Biosensor and Bioelectronic,* http://dx.doi.org/10.1016/j.bios.2017.07.042

A sensitive photoelectrochemical immunoassay of N^6-methyladenosine based on dual-signal amplification strategy: Ru doped in SiO_2 nanosphere and carboxylated g-C_3N_4

Haiyan Wang [a], Chunling Qi [b], Wenhuan He [a], Minghui Wang [a], Wenjing Jiang [a], Huanshun Yin [a,*], Shiyun Ai [a,*]

a College of Chemistry and Material Science, Shandong Agricultural University, Taian 271018, PR China

b Taian City Central Hospital Clinical Test Center, Taian, 271018, PR China

yinhs@sdau.edu.cn (Huanshun Yin)

ashy@sdau.edu.cn (Shiyun Ai)

*Corresponding author.

Abstract: A novel, simple and sensitive photoelectrochemical (PEC) immunosensing platform was constructed for detecting N^6-methyladenosine (m^6A) based on the carboxylated CN and avidin functionalized Ru@SiO_2 (ARS) nanocomposite. Herein, the N^6-methyladenosine-5′-triphosphate (m^6ATP) was selected as the detection target

molecule, m^6A antibody was used as recognition unit for m^6A, the carboxylated g-C_3N_4 (CN) was not only used as the photoactive substance, but the substrate for the m^6A antibody immobilization, ARS was synthesized and used as signal amplification unit to improve the photocurrent of CN, Phos-tag-biotin was employed as bridge of m^6ATP and Ru@SiO_2 through the specific interaction between phosphate group of m^6ATP and Phos-tag, biotin and avidin, respectively. Under the optimal condition, the fabricated PEC biosensor showed a linear range of 0.01-10 nM and high detection sensitivity with low detection limit of 3.23 pM for m^6ATP. Besides, the developed strategy was also successfully applied to evaluate the content of m^6A in human serum samples.

Keywords: N^6-methyladenosine; Ru@SiO_2; Carboxylated g-C_3N_4; Phos-tag-biotin.

1. Introduction

Over 100 distinct modifications have been discovered in cellular mRNA, tRNA, and rRNA (Globisch et al. 2011). Among these modifications, N^6-methyladenosine (m^6A) has been identified as the most frequent internal mRNA modification in all higher eukaryotes (Jia et al. 2013) and viruses (Saneyoshi et al. 1969). According to recent reports, the m^6A modification is associated with mRNA splicing, export, stability, and immune tolerance (Bokar et al. 2005). Up to now, a few methods for m^6A detection have been reported, mainly including thin layer chromatography (Grosjean et al. 2007), gas chromatography (Kellner et al. 2010), column liquid chromatography (Dubin et al. 1975), liquid chromatography coupled with mass spectrometry (Crain et al. 1998), capillary electrophoresis (Liebich et al. 2005). Though the above-mentioned approaches have great effective for detecting m^6A, some disadvantages are still existence. For example, thin layer chromatography approaches rely on incorporation ^{32}P or other radioactive labels. In gas chromatography, sample preparation of nucleic acids must include a derivatization reaction to mask polar functional groups in order to avoid thermal decomposition when the analyte is vaporized and so on. Thus, it is necessary to develop a sensitive, simple, and economical method for m^6A detection.

Photoelectrochemical (PEC) biosensor, as an emerging analytical technique, has received a great deal of attentions and undergone rapid development in recent years due to their desirable properties and attractive potential in bioassays. To date, PEC biosensor has a broad range of analytical targets, including cells (Li et al. 2016 ; Liu

et al. 2015; Pang et al. 2016; Wang et al. 2016) metal ions (Han et al. 2015), small molecules (Zhang et al. 2016), DNA (Zang et al. 2016), and proteins (Ma et al. 2016; Tu et al. 2016). In our earlier works, PEC immunosensor was fabricated based on 3-mercaptopropionic acid stabilized CdS/reduced graphene oxide nanocomposites for indole-3-acetic acid detection (Sun et al. 2014). More recently, PEC immunosensor was developed based on gold nanoparticles-functionalized g-C_3N_4 (CN) and anti-DNA:RNA antibody for microRNA detection (Yin et al. 2016), based on CN and CdS quantum dots for M. SssI methyltransferase activity analysis and inhibitor screening (Wang et al. 2017). Though the above results demonstrate that the PEC biosensor has potential to detect the biomolecule, there are still much room for improvement, such as the sensitivity of the PEC biosensor and the toxicity of photoactive substance.

As the key unit of PEC biosensor, multiple photoactive materials have been utilized in the PEC assay, including TiO_2 (Fan et al. 2016), CdS (Wang et al. 2017; Lin et al. 2016), ZnSe (Tu et al. 2016), Bi_2S_3 (Yang et al. 2015; Shu et al. 2016), and CN (Li et al. 2017; Wang et al. 2017; Lv et al. 2017; Lin et al. 2017). Particularly, CN, as a metal-free and inorganic polymeric semiconductor material, has received worldwide attention due to the unique structure and the excellent properties. CN only consists of carbon and nitrogen atoms and the band gap is 2.76 eV, resulting in the outstanding photoactivity with visible light irradiation and nontoxicity (Zhang et al. 2017). However, the photocatalytic performance CN is still limited due to the high recombination rate of electron-hole.

The organic small molecule $[Ru(bpy)_3]^{2+}$ has the unique advantage in PEC bioassay, because $Ru(bpy)_3^{2+}$ could act as both electron donor and acceptor (Zhao et al. 2014; Abruna et al. 1982; Piper et al. 2010; Guo et al. 2017). Thus, in this work, $Ru(bpy)_3^{2+}$ doped in SiO_2 (RS) was fabricated for improving the PEC response of CN. When $Ru(bpy)_3^{2+}$ absorbed optical energy, Ru^{2+} was brought up to the excited state. The Ru^{3+} species were then generated with injection of the excited electrons into the conduction band of the CN. The sacrificial electron donor ascorbic acid (AA) reduced Ru^{3+} back to Ru^{2+} and presented the continuous photocurrent. Therefore, the capture of RS could effectively reduce electron-hole recombination of CN, achieving the photocurrent enhancement. More importantly, SiO_2 with the hollow structure could load more $Ru(bpy)_3^{2+}$, resulting in the PEC response improved furthest.

Besides, phosphate-binding-tag (Phos-tag) molecule is a kind of dinuclear metal complex, which can specifically bind with phosphate group at neutral pH (Hunter et al. 1995). To date, Phos-tag has been widely used to separate and detect the large phosphoproteins (Cui et al. 2017; Kinoshita et al. 2013). Our group also proposed a electrochemical immunosensor for assay of 5-hydroxymethylcytosine (Yang et al. 2015) and protein kinase activity (Yin et al. 2016) based on Phos-tag. Thus, Phos-tag was applied to detect the m^6A as link unit due to the specifically binding ability of Phos-tag towards 5'-phosphorylated ATP. Owing to it, the PEC biosensor showed a high specificity and sensitivity. In order to evaluate the clinical applicability of the developed PEC immunosensor, the m^6A contents in the serum samples of cancer patient and healthy human were investigated.

2. Experimental

2.1 Materials and reagents

N^6-methyladenosine-5'-triphosphate (m^6ATP) was purchased from TriLink BioTechnologies, Inc. (San Diego, USA). RNase A was obtained from NEB (USA). Disodium ethylenediaminetetraacetic acid (EDTA), ascorbic acid (AA) and tris (hydroxymethyl) aminomethane (Tris) were provided by Aladdin (Shanghai, China). Diethypyrocarbonate (DEPC) was supplied by Solarbio (China). Anti-N^6-methyladenosine (m^6A) antibody, epinephrine and cortisol were from Abcam (USA). Biotinylated Phos-tag™ (Phos-tag-biotin) was provided by Wako Pure Chemical Industries, Ltd. (Japan). Avidin was supplied by Sangon Biotech (Shanghai) Co., Ltd. Tris(2, 2′-bipyridyl)dichlororuthenium(II) hexahydrate ($Ru(bpy)_3Cl_2$, $6H_2O$), Triton X-100 (TX-100) and bovine serum albumin (BSA) were provided from Sigma-Aldrich (USA). Tetraethyl orthosilicate (TEOS), 1-hexanol and cyclohexane were obtained from Beijing Yili Chemical Reagent Factory (Beijing, China). ITO conductive glass was purchased from Zhuhai Kaivo Electronic Components Co. Ltd., (China, ITO coating 180 ± 25 nm, sheet resistance <15 Ω/cm^2). Healthy human serum, breast cancer patient and gastric cancer patient serum samples were supplied by Taian Center Hospital (Shandong, China).

The buffer solutions used in this work were as follows. TE buffer, 10 mM Tris–HCl, 1 mM EDTA, pH 8.0. Phos-tag-biotin reaction buffer, 10 mM Tris-HCl (pH 7.0) containing 0.1 M NaCl, 0.1% Tween-20, 0.4 mM $Zn(NO_3)_2$. Avidin reaction buffer, 10 mM phosphate buffer saline (PBS, pH 7.4). Anti-m^6A antibody buffer, 10 mM PBS

(pH 7.4) containing 0.02% NaN_3. Washing buffer, 10 mM PBS (pH 7.4). 10 mM PBS (pH 7.4) was prepared by mixing the stock solution of 10 mM Na_2HPO_4 and 10 mM NaH_2PO_4. The pH was adjusted by 1 M HCl or 1 M NaOH. PEC determination buffer, 0.1 M PBS (pH 7.4) containing 0.1 M AA. The redistilled deionized water used in this work was treated with DEPC. The transmission electron microscopy (TEM) image of the material was acquired on a JEM-2010 transmission electron microscope (Japan).

2.2 Preparation of carboxylated CN and RS nanocomposite

CN was prepared completely according to previous paper (Wang et at. 2017). Then, 1 g CN powder and 100 mL of 5 M HNO_3 were successively placed in round bottom flask and stirred at 125 °C for 24 h (Chen et al. 2013). Followed, a suspending liquid was centrifuged and the sediment was collected and washed with double distilled deionized water. Finally, the obtained product was drying at 60 ^oC for 2 h and stored for further use.

RS nanocomposite was synthesized according to previous report with some modifications. 1.77 mL TX-100, 7.5 mL cyclohexane, 1.8 mL 1-hexanol and 340 μL water were firstly mixed. Then 80 μL of 0.1 M $Ru(bpy)_3^{2+}$ aqueous solution 100 μL of TEOS and 60 μL NH_4OH (25%) were successively added into the mixture. After stirring for 24 h, 50 mL acetone was added into the above solution and the sediment was collected. Subsequently, the obtained product was washed with ethanol and double distilled deionized water for three times to remove any surfactant molecules. After dried at 60 °C for 12 h, the orange RS nanocomposite was obtained. Then, 1 mg RS nanocomposite was dispersed in 1 mL of 10 mM PBS (pH 7.4) and activated by

0.5 mL of 0.1 M PBS (pH 7.4) containing EDC (0.5 mg/mL) and NHS (0.5 mg/mL) for 0.5 h. Followed, 1 mL of 0.1 mg/mL avidin was added into the above solution and incubated for 1 h. The ARS bioconjugate was finally obtained after centrifugation. It was dispersed in 1 mL of 10 mM PBS (pH 7.4), and it was stored at 4 °C for further use .

2.3 PEC immunosensor fabrication

The ITO conductive glass was first cut into 5.0×1.0 cm^2 pieces and sonicated respectively in ethanol/NaOH mixed solution (v/v, 1:1), acetone and double distilled deionized water for 30 min, followed by drying at 60 ^oC for 2 h. For fabricating PEC immunosensor, 20 μL of 1 mg/mL CN dispersion was activated by 20 μL of 0.1 M PBS (pH 7.4) containing EDC (0.5 mg/mL) and NHS (0.5 mg/mL) for 0.5 h. Subsequently, the activated CN dispersion was dropped on a bare ITO electrode surface and dried under infrared lamp irradiation. After the obtained CN/ITO electrode was washed with double distilled deionized water for three times, 20 μL of 10 mM PBS (pH 7.4) containing 10 μg/mL m^6A antibody was further dropped on the ITO electrode surface and incubated for 60 min at 37 °C in a humid environment. For the purpose of blocking the nonspecific binding sites, the electrode was incubated in 1% BSA solution at room temperature for 1 h and then washed with washing buffer for three times, noted as Ab/CN/ITO. Afterwards, the obtained Ab/CN/ITO electrode was incubated with 20 μL of 10 mM PBS (pH 7.4) containing different concentrations of m^6ATP for 60 min at 37 °C under humid environment. Then, the electrode was rinsed with washing buffer for three times and noted as $m^6ATP/Ab/C_3N_4/ITO$. Next, 20 μL

of Phos-tag-biotin reaction buffer containing 10 μM Phos-tag-biotin was dripped on the electrode (m^6ATP/Ab/CN/ITO) surface and incubated for 1 h in a humidified chamber. After washed with washing buffer for three times, the electrode (Phos-tag/m^6ATP/Ab/CN/ITO) was further incubated with 20 μL ARS bioconjugate dispersion for 50 min at 37 °C in a humidified chamber followed by rinsing with washing buffer for three times. The electrode was named as ARS /Phos-tag/m^6ATP/Ab/CN/ITO. In addition, ARS dispersion was firstly dropped on a bare ITO electrode and CN/ITO electrode surface respectively, and then dried under infrared lamp irradiation. The fabricated electrodes were note as ARS/ITO and ARS/CN/ITO respectively.

2.4 PEC detection

PEC measurements were performed with a homemade PEC system with visible light. A 500 W Xe lamp was used as the irradiation source to produce visible-light (light intensity was 20 mW/cm^2). The photocurrent was recorded with a CHI832A electrochemical workstation (CHI instruments, Austin, USA) with a conventional three-electrode system in PBS (0.1 M, pH 7.0) containing 0.1 M AA, which was deaerated by nitrogen for 30 min before experiments. A modified ITO electrode was used as the working electrode, a Pt wire and a saturated calomel electrode (SCE) were used as the counter electrode and the reference electrode, respectively.

Electrochemical impedance spectroscopy (EIS) was carried out with a CHI660C electrochemical workstation (CHI instruments, Austin, USA) in 10 mM PBS containing 5.0 mM $Fe(CN)_6^{3-/4-}$ (1:1) and 0.1 M KCl (pH 7.4) with the frequency

range of 10^{-1}- 10^{5} Hz.

3. Results and discussion

3.1. Detection strategy of the PEC biosensor

Scheme 1

In this work, a novel PEC immunosensor was proposed for m^6A assay, based on the specific recognition effect of Phos-tag-biotin towards phosphate group of m^6ATP, the bioaffinity reaction between avidin and biotin, the immunoreaction between anti-m^6A antibody and m^6ATP, where carboxylated CN was used as photoactivity substances, ARS was used as signal amplification unit. As shown in Scheme 1, carboxylated CN was firstly coated on the bare ITO electrode surface through physical adsorption, where the CN was not only as photoactivity substance, but also as a bridge for antibody immobilization. Based on the chemical reaction between carboxyl group of CN and amino group of m^6A antibody, the m^6A antibody was attached on the above electrode surface. Subsequently, through the immunoreaction between antigen and antibody, m^6ATP could be further assembled, where the phosphate group of m^6ATP was away from the ITO surface. Afterwards, Phos-tag-biotin could be captured on the ITO electrode surface based on the phosphate group identification ability of Phos-tag. Then, ARS was introduced to ITO electrode surface, which was achieved by the specific reaction between biotin and avidin. In fact, in this work, SiO_2 was used as the carrier of $Ru(bpy)_3^{2+}$, and the $Ru(bpy)_3^{2+}$ was utilized as the signal amplification unit. There were two ways for enhancing the photocurrent by $Ru(bpy)_3^{2+}$: (1) when the

$Ru(bpy)_3^{2+}$ absorbed optical energy, the electrons were excited. The Ru^{3+} species produced when the excited electrons injected into the conduction band of the CN. The sacrificial electron donor AA reduced Ru^{3+} back to Ru^{2+} and presented the continuous photocurrent. (2) The excited electrons of Ru^{2+} transferred into the conduction band of the ITO electrode surface directly and the Ru^{3+} produced. Then, with AA donating the electron, the Ru^{3+} was transformed into Ru^{2+} and the photocurrent sustained. Thus, with the immobilization of ARS, photocurrent intensity of the immunosensor had a great enhancement, and the schematic illustration of the photocurrent enhancement mechanism was displayed in Fig. S1. According to the relationship between the photocurrent response and the m^6ATP concentration, the m^6ATP detection could be achieved.

3.2 Characterization of carboxylated CN and ARS

Figure 1

The morphology of carboxylated CN was characterized by TEM. Fig. 1A showed the TEM image of the prepared carboxylated CN, illustrating the nanosheet structure. The X-ray diffraction patterns (XRD) of CN and carboxylated CN were presented in Fig. 1B. Two peaks were presented for CN, confirming a graphitic-like layer structure. The strong peak at 27.6° was the characteristic of the stacking peak of conjugated aromatic system and indexed to the (002) plane of graphitic materials. The peak at 13.12° was assigned to the (100) plane of CN and indexed to an in-plane structural packing motif. After the carboxyl process of CN, the (100) peak almost

disappeared. Therefore, the XRD patterns of carboxylated CN indicated that the lattice structure of CN was not altered after the carboxyl process, which was beneficial for fabricating PEC immunosensor. Fig. 1C showed the prepared ARS nanocomposites with the size of ~40 nm, which was consummate for fabricating biosensor. In order to further verify the successful preparation of ARS, the electrochemiluminescence (ECL) of ARS was measured by the MPI-E ECL analyzer from Xi'an Remax Electronic Science & Technology Co. Ltd. (Xi'an, China). As can been seen in Fig. 1D, a strong ECL response was obtained, indicating $Ru(bpy)_3^{2+}$ doped in SiO_2 nanoparticles successfully.

3.3. EIS characterization

Figure 2

The stepwise fabrication process of the PEC immunosensor was characterized by electrochemical impedance spectroscopy (EIS) in 5 mM $Fe(CN)_6^{3-/4-}$ (1:1) solution. As shown in Fig. 2A, the bare ITO electrode showed an electron transfer impedance (R_{et}) of about 40 Ω (curve a). After the carboxylated CN was coated on the ITO electrode, a semi-circle with a R_{et} of about 70 Ω was obtained (curve b), which could be ascribed that the diffusion efficiency of the redox probe to electrode was hindered, due to the negative charge efficiency of carboxyl group. Subsequently, the R_{et} value was increased significantly when m^6A antibody was captured on the electrode surface (curve c). Obviously, the increased R_{et} was caused by the immobilization of antibody with high volume and insulativity, the diffusion of the redox probe was hindered by

the huge volume of antibody. After the capture of m^6ATP, the R_{et} value was further increased, which could be explained as the introduction of the phosphate group with two negative charges, blocking the diffusion of the redox probe of $Fe(CN)_6^{3-/4-}$ to electrode surface (curve d). Afterwards, due to the insulating effect of biomolecule, the R_{et} increased greatly when the Phos-tag-biotin was successfully captured by the phosphate group of m^6ATP (curve e). Finally, the ARS was conjugated with Phos-tag-biotin on the electrode surface based on the specific reaction between avidin and biotin, the obtained R_{et} was increased further (curve f), which could also be attributed to the fact that the ARS with a large size could impede the migration of redox probe towards electrode surface. Based on the above results, the successfully fabrication of the biosensor can be confirmed.

3.4. Detection feasibility assay

In order to testify the detection feasibility of the biosensor, the photocurrents of ITO electrode with different modifications were recorded and compared in 0.1 M PBS containing 0.1 M AA under visible light irradiation, where AA was employed as electron donor. As can been seen from Fig. 2B, no photocurrent response was observed at the bare ITO electrode (curve a). After the coating of carboxylated CN and ARS on ITO electrode respectively, the obtained photocurrent responses were both significant, indicating the commendably photoelectric activity of carboxylated CN (curve b) and ARS (curve c). Nevertheless, when ARS was directly modified on CN/ITO electrode, a stronger photocurrent response was obtained (curve d). It clearly demonstrated that ARS as signal multiplication unit could enhance the PEC response

of carboxylated CN. When the CN/ITO was incubated with m^6A antibody, m^6ATP, Phos-tag-biotin successively, the observed PEC responses slightly decreased (curve e) compared with the photocurrent of CN/ITO. It could be attributed that those biomolecules had no response upon light irradiation and blocked the electron diffusion of AA to the electrode surface. Finally, a strong photocurrent closed to the photocurrent of ARS/CN/ITO was obtained when the ARS was captured (curve f) through the specific reaction between avidin and biotin. In order to further testify this feasibility of this assay, the CN/ITO was incubated with m^6A antibody, m^6ATP, Phos-tag-biotin, ARS, successively. The obtained PEC response (curve g) was closed to the photocurrent of CN/ITO, indicating the absence of the signal amplification unit. According to the above results, we could confirm that the developed PEC biosensor could be applied to detect m^6ATP.

3.5. Optimization of detection conditions

Figure 3

In order to acquire an optimal PEC response, several parameters were optimized，including concentration of CN and antibody, immunoreaction time and temperature, Phos-tag-biotin concentration and ARS immobilization time.

As shown in Fig. 3A, the photocurrent increased with the CN concentrations increasing from 0.2 to 1.0 mg/mL and reached a maximum at 1.0 mg/mL. When the CN concentration was further increased, the photocurrent response decreased, indicating that thicker CN was unprofitable for the charge transportation rate. Thus,

1.0 mg/mL CN solution was selected as the optimal concentration.

As can be seen in Fig. 3B, the photocurrent increased obviously with the m^6A antibody concentration increased from 0.01 to 10 μg/ml, and then the PEC response increased slowly when further increasing the m^6A antibody concentration. Therefore, 10 μg/ml was the optimum antibody concentration for this PEC biosensor.

In order to obtain satisfactory detection efficiency, the immunoreaction time for m^6A antibody (10 μg/mL) and m^6ATP (10 nM) was also investigated in this work. Fig. 3C illuminated the effects of immunoreaction time on the PEC response of the immunosensor. With the immunoreaction time extending from 10 to 60 min, the PEC response increased quickly and tended to level off when further prolonging the reaction time to 70 min. Thus, 60 min was used as the immunoreaction in this work. As revealed in Fig. 3D, the photocurrent increased along with the increasing temperature and fell drastically after 37 ^oC. Thus, the immunoreaction temperature was optimized to 37 ^oC.

The Phos-tag-biotin was acted as a 'bridge' to link phosphate group and ARS, the concentration was investigated. As shown in Fig. 3E, the PEC response of the immunosensor increased obviously with Phos-tag-biotin concentration from 1 to 10 nM, suggesting that more Phos-tag-biotin was captured on the ITO electrode surface with high concentration, and leaded to a stronger photocurrent signal. However, when the Phos-tag-biotin concentration was further increased to 20 nM, the obtained PEC response tended to level off. Thus, 10 nM was a considerable concentration.

ARS was used as the signal amplification unit and immobilized onto the ITO

surface through the combination between the Phos-tag-biotin and avidin. The immobilization time of the ARS was explored and shown in Fig. 3F. The optimal immobilization of 50 min was employed. Besides, the concentration of AA was also optimized and the result was presented in Fig. S2.

3.6 Analytical performance

Figure 4

Under the optimal conditions, the PEC response of the prepared immunosensor was examined with different concentrations of m^6ATP. As can been seen in Fig. 4A, the photocurrent increased gradually along with changing the m^6ATP concentration from 0.01 to 10 nM. And the logarithm values of the m^6ATP concentration from 0.01 to 10 nM were proportional to the photocurrent and the calibration curve was present in Fig. 4B. The linear regression equation is I(μA)=0.2395log$c$(nM)+0.559 (S/N=3, R=0.9984) and the detection limit was estimated to be 3.23 pM. The detection limit of our work was lower than other methods such as electrochemiluminescence with the detection limit of 0.77 nM (Lin et al. 2010) and high-performance liquid chromatography with the detection limit of 7 nM (Xu et al. 2000). The obtained results illustrated that the PEC immunosensor was achievable to monitor the m^6ATP.

The selectivity is one of the key parameters for the PEC biosensor. ATP, dATP, epinephrine and cortisol were selected as interferents to investigate the selectivity of the immunosensor for detecting m^6ATP. As revealed in Fig. 4C, after the m^6ATP replacing with interferents, the photocurrent was lower than that obtained for m^6ATP and it was close to the photocurrent of CN/ITO. Thus, the developed PEC biosensor

showed a good selectivity for m^6ATP detection.

The reproducibility of the PEC biosensor was evaluated by measuring the m^6ATP at 10 nM with six parallel immunosensors. The relative standard deviation for six determinations was 4.21% (Fig. 4D), indicating acceptable detection reproducibility. The stability of the immunoassay system was investigated after stored at 4 ^oC for one week and the photocurrents remained 92.35% of its original photocurrent.

3.7 Real sample analysis

Figure 5

According to recent discovery, the abnormal expression of m^6A was closely associated with cancer, indicating that m^6A could be as a valuable new cancer biomarker for early diagnosis and prognostics (Meyer et al. 2014). Thus, the content of m^6A in serums of breast cancer patient and gastric cancer patient were detected and compared with m^6ATP content in healthy human serums. For obtaining the oligonucleotides containing m^6ATP, the total RNA was firstly extracted from the three kinds of serums by miRNeasy Serum/Plasma Kit (Qiagen, Germany). Subsequently, the three kinds of total RNA concentration was detected and diluted into the same concentration. Then, the diluent of the total RNA was treating with 100 μg/mL RNase A for 2 h at 37 °C. Then, under the optimal experimental conditions, 20 μL of the obtained oligonucleotides was assembled onto the PEC biosensor and detected. As can be shown in Fig. 5, the PEC responses of the breast cancer and gastric cancer serums were higher than that of healthy human serums, which was in accordance with

the detection results obtained from EpiQuik m^6A RNA Methylation Quantification Kit (Epigentek, USA). It was also denoted that the expression level of m^6A in cancer serums were higher than that in healthy human serum. Thus, on the base of these results, we can conclude that this detection strategy has the ability to detect m^6A in real samples.

4. Conclusion

In summary, a novel PEC immunosensor was successfully developed for m^6A detection using the carboxylated CN as the substance for immobilizing m^6A antibody and the photoactive material, ARS as signal amplification unit. Upon the light illumination, the photocurrent enhancement of CN was achieved in AA solution, which acted as the electron donor for Ru^{3+} generated from interfacial electron injection of photoexcited Ru^{2+}. Moreover, the sensitivity and specificity of the PEC biosensor was improved by the specific interaction between Phos-tag and phosphate group, biotin and avidin. Importantly, the developed PEC biosensor was successfully used to detect m^6A in biological samples with a high correctness, demonstrating the PEC immunosensor could be employed as a new trustworthy strategy for the m^6A detection.

Acknowledgements

This work was supported by the Natural Science Foundation of Shandong province China (Nos. ZR2016BM10, ZR2014BQ029), the National Natural Science Foundation of China (No. 21375079) and China Postdoctoral Science Foundation (Nos. 2015T80732 and 2015M582120).

References

Abruna, H.D., Bard, A.J., 1982. J Am. Chem.Soc. 104, 2641-2642.

Bokar, J. A., 2005. Springer Berlin Heidelberg 141-177.

Chen, L., Huang, D., Ren, S., Dong, T., Chi, Y., Chen, G., 2013. Nanoscale 5, 225-230.

Cui, L., Lu, M., Yang, X. Y., 2017. Analyst 142, 1562-1568.

Guo, W., Cao, Z., Liu, Y., Su, B., 2017. ChemElectroChem.

Crain, P. F., 1998. Am. Soc. Microbiol Press 47-57.

Dubin, D.T., Taylor, R. H., 1975. Nucleic Acids Res. 2, 1653-1668.

Fan, G.C., Zhu, H., Du, D., Zhang, J. R., Zhu, J. J., Lin, Y., 2016. Anal. Chem. 88 3392-3399.

Globisch, D., Pearson, D., Hienzsch, A., Brückl, T., Wagner, M., Thoma, I., Sieber, S. A., 2011. Angew. Chem. Int. Ed. 50, 9739-9742.

Grosjean, H., Droogmans, L., Roovers, M., Keith, G., 2007. Methods Enzymol. 425, 55-101.

Han, D.M., Jiang, L. Y., Tang, W. Y., Xu, J. J., Chen, H. Y., 2015. Electrochem. Commun. 51, 72-75.

Hunter, 1995. Cell 80, 225-236..

Jia, G., Fu, Y., He, C., 2013. Trends Genet. 29, 108-115.

Kellner, S., Burhenne, J., Helm, M., 2010. RNA Biol. 7, 237-247.

Kinoshita, E., Kinoshita-Kikuta, E., Koike, T., 2013. Anal. Biochem. 438, 104-106.

Li, L., Zhang, Y., Zhang, L., Ge, S., Liu, H., Ren, N., Yu, J., 2016. Anal. Chem. 88, 5369-5377.

Li, X., Zhu, L., Zhou, Y., Yin, H., Ai, S., 2017. Anal. Chem. 89, 2369-2376.

Liebich, H.M.M.-H., S. Klaus, F., 2005. J Chromatogr A 1071, 271-275.

Lin, Y., Zhou, Q., Tang, D., Niessner, R., Knopp, D., 2017. Anal. Chem. 89, 5637-5645.

Lin, Z., Wang, W., Jiang, Y., Qiu, B., Chen, G., 2010. Electrochim. Acta 56, 644-648.

Liu, H., Weng, L., Yang, C., 2017. Microchim. Acta, 1-17.

Liu, S., Cao, H., Wang, Z., Tu, W., Dai, Z., 2015. Chem. Commun. 51, 14259-14262.

Lv, S., Zhang, K., Lin, Z., Tang, D., 2017. Biosens. Bioelectron. 96, 317-323.

Ma, Z.Y., Ruan, Y. F., Xu, F., Zhao, W. W., Xu, J. J., Chen, H. Y., 2016, Anal. Chem. 88, 3864-3871.

Meyer, K.D., Jaffrey, S. R., 2014. Nat. Rev. Mol. Cell Biol. 15, 313-326.

Pang, X., Zhang, Y., Pan, J., Zhao, Y., Chen, Y., Ren, X., Du, B., 2016. Biosens. Bioelectron. 77, 330-338.

Piper, D.J., Barbante, G.J., Brack, N., Pigram, P.J., Hogan, C.F., 2010. Langmuir 27, 474-480.

Saneyoshi, M., Harada, F., Nishimura, S., 1969. Biochim. Biophys. Acta 190, 264-273.

Shu, J., Qiu, Z., Lin, Z., Cai, G., Yang, H., Tang, D., 2016. Anal. Chem. 88, 12539-12546.

Sun, B., Chen, L., Xu, Y., Liu, M., Yin, H., Ai, S., 2014. Biosens. Bioelectron. 51,

164-169.

Tu, W., Cao, H., Zhang, L., Bao, J., Liu, X., Dai, Z., 2016. Anal. Chem. 88, 10459-10465.

Wang, H., Liu, P., Jiang, W., Li, X., Yin, H., Ai, S., 2017. Sens. Actuators B: Chem. 244, 458–465.

Wang, Y. Z., Hao, N., Feng, Q. M., Shi, H. W., Xu, J. J., Chen, H. Y., 2016. Biosens. Bioelectron. 77, 76-82.

Xu, G., Schmid, H. R., Lu, X., Liebich, H. M., Lu, P., 2000. Biomed. Chromatogr. 14, 459-463.

Yang, Z., Wang, F., Wang, M., Yin, H., Ai, S., 2015. Biosens. Bioelectron. 66, 109-114.

Yin, H., Zhou, Y., Li, B., Li, X., Yang, Z., Ai, S., Zhang, X., 2016. Sens. Actuators B: Chem 222, 1119-1126.

Zang, Y., Lei, J., Hao, Q., Ju, H., 2016. Biosens. Bioelectron. 77, 557-564.

Zhang, K., Lv, S., Lin, Z., Tang, D., 2017. Biosens. Bioelectron. 95, 34-40.

Zhang, N., Ruan, Y. F., Ma, Z. Y., Zhao, W. W., Xu, J. J., Chen, H. Y., 2016. Biosens. Bioelectron. 85, 294-299.

Zhao, W.W., Xu, J. J., Chen, H. Y., 2014. Chem. Rev. 114, 7421-7441.

Figure captions

Scheme 1. (A) Preparation of avidin-Ru@SiO_2. (B) Schematic illustration of PEC biosensor fabrication.

Fig. 1 (A) TEM images of carboxylated CN. (B) XRD of CN (a) and carboxylated CN (b). (C) TEM image of avidin-Ru@SiO_2 nanocomposites. (D) The ECL response of the avidin-Ru@SiO_2/ITO in 0.1 M $S_2O_8^{2-}$ solution.

Fig. 2 (A) Nyquist diagrams of EIS recorded from 10^{-1} Hz to 10^5 Hz in $Fe(CN)_6^{3-4-}$ (5 mM, 1:1) solution containing 0.1 M KCl at different electrodes. (a) ITO, (b) C_3N_4/ITO, (c) Ab/C_3N_4/ITO, (d) m^6ATP/Ab/C_3N_4/ITO, (e) Phos-tag/m^6ATP/Ab/C_3N_4/ITO, (f) avidin-Ru@SiO_2/Phos-tag/m^6ATP/Ab/C_3N_4/ITO. (B) The PEC response of different electrode in 0.1 M PBS containing 0.1 M AA. (a) bare ITO, (b) C_3N_4/ITO, (c) Ru@SiO_2/ITO, (d) Ru@SiO_2/C_3N_4/ITO, (e) Phos-tag/m^6ATP/Ab/C_3N_4/ITO, (f) Ru@SiO_2/Phos-tag/m^6ATP/Ab/C_3N_4/ITO, (g) C_3N_4/ITO treated successively with m^6A antibody, Phos-tag-biotin, avidin-Ru@SiO_2.

Fig. 3 Effects of CN (A) and antibody (B) concentration, immunoreaction time (C) and temperature (D) for m^6A antibody and m^6ATP, Phos-tag-biotin concentration (E)

and avidin-Ru@SiO_2 immobilization time (F) on the PEC response. The error bars represent the standard deviation of three measurements.

Fig. 4 (A) The photocurrent of the biosensor with different concentrations of m^6ATP. (a–j) 0.01, 0.02, 0.03, 0.05, 0.1, 1, 5, 10, 20, 30 nM. (B) Calibration curve. (C) The photocurrent change of the biosensor after it was incubated with (from A to E) 10 nM m^6ATP, 10 nM ATP, 10 nM dATP, 10 μg/ml epinephrine, 10 μg/ml cortisol, respectively. (D) The reproducibility for the PEC response of six biosensors fabricated dependently.

Fig. 5 The relative expression of m^6A in different serums. The error bars represent the standard deviation of three measurements.

Graphic Abstract

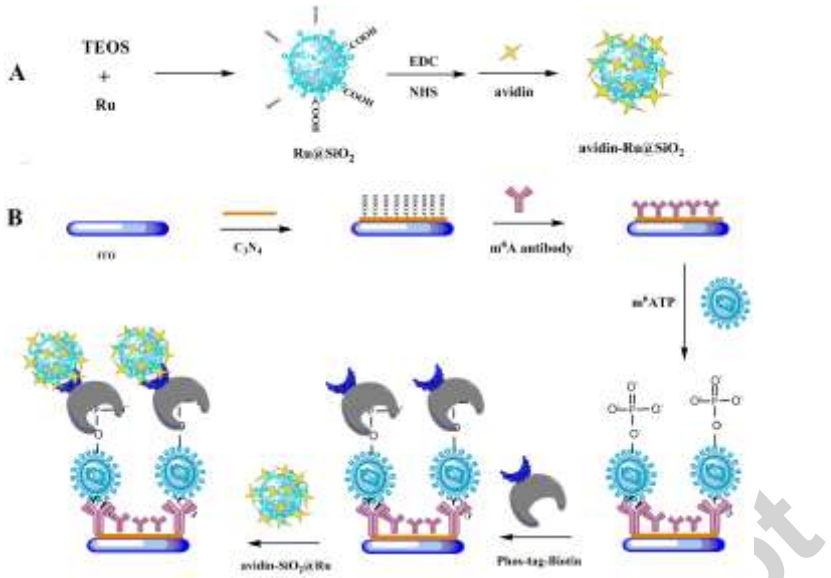

Highlights

- A photoelectrochemical strategy was developed for N^6 -methyladenosinedetection.
- Rudoped in SiO_2 nanosphere and carboxylated g-C_3N_4were used as photoactive materials.
- Phos-tag-biotin was employed as bridge of m^6ATP and Ru@SiO_2.
- The photoelectrochemical immunosensor was validated for detecting m^6A content incancer patientsblood serum.

Fig. 1

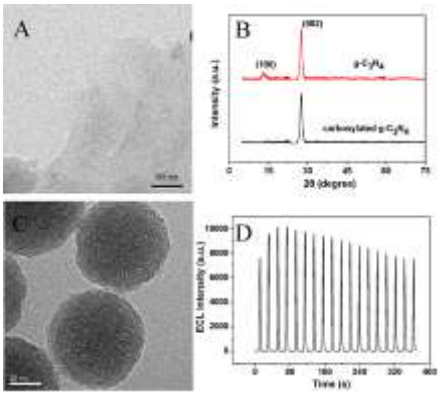

Fig. 2

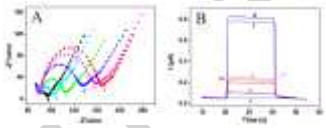

Fig. 3

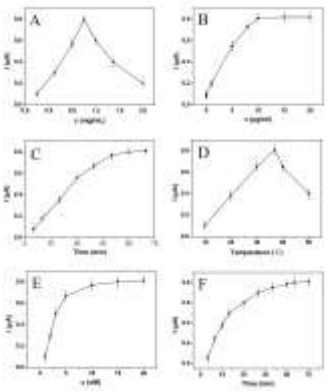

Fig. 4

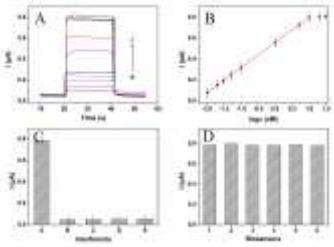

Fig. 5

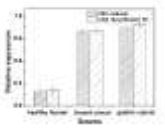

Sc. 1